SPEEDAM 2008
International Symposium on Power Electronics,
Electrical Drives, Automation and Motion

Comparison of Low-Cost-Implementation Sensorless Schemes in Vector Controlled Adjustable Speed Drives

M. Cacciato*, G. Scarcella*, G. Scelba*, S. M. Billè**, D. Costanzo**, A. Cucuccio**
* DIEES – UNIVERSITY OF CATANIA, Viale A. Doria, 6 95125, CATANIA, ITALY
** ST Microelectronics CATANIA, Stradale Primosole, CATANIA ITALY

***Abstract*-- The paper describes the comparison between different high-performance low-cost-implementation techniques for the estimation of the rotor flux in medium-high speed sinusoidal AC motor drives. In sensorless estimation, rotor flux is estimated from measured terminal voltages and currents, and is used as a feedback in vector control schemes, achieving almost the same high-performance of sensored drives. At high speed, a key point is the robustness at parameter variations of estimators, which use only integration and feedback summation and observers that use more complex approximate differentiation. The paper points out some implementation differences between a classical open loop rotor flux estimator based on the voltage model, and a more complex Luenberger rotor flux observer when a low cost high performance STM32 microcontroller of ST Microelectronics, is used. Comparison of these two schemes is performed either in simulation and experimentally.**

***Index Terms*—sensorless vector control, rotor flux observers, discrete time domain.**

I. INTRODUCTION

In the past, Adjustable Speed Drives (ASD) that have been used for applications requiring medium-low dynamic performance, like fans, pumps have been typically based on Voltage Source Inverters (VSIs) with scalar controllers like constant V/f or slip control [1], [2]. Vector control schemes, that include closed loop current control and speed feedback, have been considered too expensive for such low-cost applications, even if the advantages of current feedback, in terms of over-current protection and improved performance in transient operation, could be of interest either to manufactures and customers of such low-cost applications. Today the market of ASD is rapidly changing due to several reasons. Measurement the current feedback that has been developed for vector control schemes, is not expensive, and can be easily achieved by using sensing resistors or other low-cost current feedback devices. Consequently, two are the requirements that have been fulfilled to equip ASD with more sophisticated controls: reduce the cost of the hardware implementation and reduce or avoid the cost of the speed feedback. Till few years ago there was a big difference in terms of size and cost between the hardware needed to implement a scalar or a vector control. The hardware gap has been rapidly filled, and, as presently there is only a minimal differences in cost and size between scalar and vector implementation, also ASD could be advantaged by the use of more powerful hardware.

Regarding the need of a shaft transducer, conventional vector controlled AC motor drives require the knowledge of the rotor flux position to orientate the stator current vector and obtain an independent control of flux and torque. According to the specific AC motor used, the instantaneous angular position of the rotor flux is usually determined by measuring the rotor position trough shaft transducers (resolvers or optical encoders). They all increase cost, sizes and circuit complexity of AC motor drives, and often reduce their reliability, as additional signal contactors and leads are required, seriously limiting any practical application. Even in case of synchronous PM motors, where the rotor flux position coincides to the rotor position, due to the synchronism between rotor flux and motor shaft, the presence of the position transducer heavily affects the total cost of the drive. In addition to rotor position estimation needed for vector control, rotor speed information is also required to close the speed loop, often present in ASD.

Reduction of hardware implementation costs and elimination of any mechanical equipment for speed or angle detection represents a practical manufacturing advantage in terms of cost and size reduction of electric drives. A sensorless vector control implemented in a low-cost hardware can replace conventional scalar control in all the low-cost application, where ASD are used. Many schemes have been proposed in literature to perform sensorless estimation of the mechanical machine quantities from the voltage and current measurements [3], [4]. They range from the simplest, that uses only the model of the machine to the more complex, that adds to the model of the machine some feedbacks (observers). Transition of these schemes to the discrete domain implemented by using low-cost hardware, is presented in literature by comparing simple and more complex estimation schemes implemented by using low cost hardware, this paper aims to answer the question: if low cost μP have to be used, it is better to implement simpler control schemes that can run faster and with low memory resources, or the complexity of the observer can be maintained like in the systems with higher calculation

978-1-4244-1664-6/08/$25.00 ©2008 IEEE

power? The paper compares a classical open loop flux estimator versus a more complex Luenberger flux observer to sensorless estimate rotor position and speed. Both schemes are implemented in a STM32 (core CORTEX-M3) microcontroller, and are been tested on Permanent Magnet Synchronous Machines (PMSMs). The results of such a comparison in terms of performance, μP computation effort, robustness to parameter variation are presented with important practical hints on implementation and voltage and current measurements.

II. Open-loop flux estimators and closed-loop flux observers for sensorless control

According to the sensorless approach, both open- and closed-loop estimator algorithms require the measurement of voltages and currents, transformed in a *q,d* stationary reference frame [3]. The equations of the most common open-loop rotor flux estimator based on the voltage model are directly deduced from the model of the machine in the stator reference frame and, by referring to an isotropic PMSM, are:

$$\begin{cases} v_{qs}^s = R_s \cdot i_{qs}^s + L_s \dfrac{di_{qs}^s}{dt} + e_{qs}^s \\ v_{ds}^s = R_s \cdot i_{ds}^s + L_s \dfrac{di_{ds}^s}{dt} + e_{ds}^s \end{cases} \tag{1}$$

where:

$$\begin{cases} e_{qs}^s = \dfrac{d\lambda_{PMqs}^s}{dt} = \omega_r \cdot \Lambda_{PM} \cdot cos(\theta_r) = \omega_r \cdot \lambda_{PMds}^s \\ e_{ds}^s = \dfrac{d\lambda_{PMds}^s}{dt} = -\omega_r \cdot \Lambda_{PM} \cdot sin(\theta_r) = -\omega_r \cdot \lambda_{PMqs}^s \end{cases} \tag{2}$$

and Λ_{PM} is the amplitude of the permanent magnet flux, $L_s$is the stator inductance, θ_r and $\omega_r$are the rotor position and speed in electrical degrees. In terms of *q,d* components of the permanent magnet flux we have:

$$\begin{cases} \lambda_{PMqs}^s = \int \left(v_{qs}^s - R_s \cdot i_{qs}^s\right) dt - L_s \cdot i_{qs}^s \\ \lambda_{PMds}^s = \int \left(v_{ds}^s - R_s \cdot i_{ds}^s\right) dt - L_s \cdot i_{ds}^s \end{cases} \tag{3}$$

In the time-discrete domain, where the notation $f_{qs}^s = f_\alpha$ and $f_{ds}^s = f_\beta$ has been used for simplicity, the estimated components of the PM flux are:

$$\begin{cases} \hat{\lambda}_{PM\alpha}(k) = \cdot \sum_{1}^{k-1} \left(v_\alpha(h) - R_s \cdot i_\alpha(h)\right) \cdot T_s - L_s \cdot i_\alpha(k) \\ \hat{\lambda}_{PM\beta}(k) = \sum_{1}^{k-1} \left(v_\beta(h) - R_s \cdot i_\beta(h)\right) \cdot T_s - L_s \cdot i_\beta(k) \end{cases} \tag{4}$$

In Fig. 1 is shown the block diagram of the estimator given by (4). Notice that the estimator is formally identical to that of an induction machine in which L_s is replaced by the total leakage inductance $L_\sigma = \left(L_s - \dfrac{L_m^2}{L_r}\right)$.

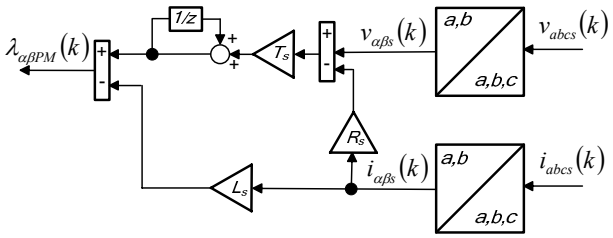

Fig. 1 -Block diagram of the open loop estimator.

In order to consider Luenberger observers the state space model of the machine is adopted:

$$\begin{cases} \dfrac{di_{qs}^s}{dt} = -\dfrac{R_s \cdot i_{qs}^s}{L_s} - \dfrac{e_{qs}^s}{L_s} + \dfrac{v_{qs}^s}{L_s} \\ \dfrac{di_{ds}^s}{dt} = -\dfrac{R_s \cdot i_{ds}^s}{L_s} - \dfrac{e_{ds}^s}{L_s} + \dfrac{v_{ds}^s}{L_s} \\ \dfrac{d\theta_r}{dt} = \omega_r \end{cases} \tag{5}$$

being $x = \left[i_{qs}^s \; i_{ds}^s \; \theta_r\right]^T$ the state vector, $u = \left[v_{qs}^s \; v_{ds}^s\right]^T$ the input vector, and $y = \left[i_{qs}^s \; i_{ds}^s\right]^T$ the output vector. By supposing the mechanical quantities slowly changing versus the electrical ones and introducing two new state variables it can be obtained:

$$\begin{cases} \dfrac{di_{qs}^s}{dt} = -\dfrac{R_s \cdot i_{qs}^s}{L_s} - \dfrac{e_{qs}^s}{L_s} + \dfrac{v_{qs}^s}{L_s} \\ \dfrac{di_{ds}^s}{dt} = -\dfrac{R_s \cdot i_{ds}^s}{L_s} - \dfrac{e_{ds}^s}{L_s} + \dfrac{v_{ds}^s}{L_s} \\ \dfrac{de_{qs}^s}{dt} = \omega_r \cdot e_{ds}^s \\ \dfrac{de_{ds}^s}{dt} = -\omega_r \cdot e_{qs}^s \end{cases} \tag{6}$$

being $x = \left[i_{qs}^s \; i_{ds}^s \; e_{qs}^s \; e_{ds}^s \right]^T$ the new state vector, $u = \left[v_{qs}^s \; v_{ds}^s \right]^T$ the input vector, and $y = \left[i_{qs}^s \; i_{ds}^s \right]^T$ the output vector. As the observer requires, (6) is considered with the estimated values $\hat{x} = \left[\hat{i}_{qs}^s \; \hat{i}_{ds}^s \; \hat{e}_{qs}^s \; \hat{e}_{ds}^s \right]^T$ and introducing a correction term $K = y - \hat{y}$, that in our case is the error between the feedback and the estimated currents. Therefore, in the time-discrete domain we obtain:

$$\begin{cases} \hat{i}_\alpha(k+1) = \hat{i}_\alpha(k) - \dfrac{R_s}{L_s} \cdot \hat{i}_\alpha(k) \cdot T_s + K_1 \cdot \left(i_\alpha(k) - \hat{i}_\alpha(k) \right) \cdot T_s + \\ - \dfrac{\hat{e}_\alpha(k)}{L_s} \cdot T_s + \dfrac{v_\alpha(k)}{L_s} \cdot T_s \\ \hat{i}_\beta(k+1) = \hat{i}_\beta(k) - \dfrac{R_s}{L_s} \cdot \hat{i}_\beta(k) \cdot T_s + K_1 \cdot \left(i_\beta(k) - \hat{i}_\beta(k) \right) \cdot T_s + \\ - \dfrac{\hat{e}_\beta(k)}{L_s} \cdot T_s + \dfrac{v_\beta(k)}{L_s} \cdot T_s \\ \hat{e}_\alpha(k+1) = \hat{e}_\alpha(k) + K_2 \cdot \left(i_\alpha(k) - \hat{i}_\alpha(k) \right) \cdot T_s + \omega_r \cdot \hat{e}_\beta(k) \cdot T_s \\ \hat{e}_\beta(k+1) = \hat{e}_\beta(k) + K_2 \cdot \left(i_\beta(k) - \hat{i}_\beta(k) \right) \cdot T_s - \omega_r \cdot \hat{e}_\alpha(k) \cdot T_s \end{cases} \quad (7)$$

where again the notation $f_{qs}^s = f_\alpha$ and $f_{ds}^s = f_\beta$ have been used. The block diagram of the observer is shown in Fig. 2.

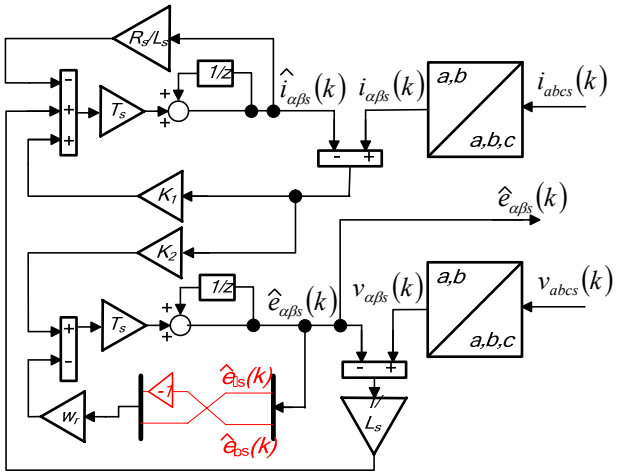

Fig. 2- Block diagram of the Luenberger observer.

A. Implementation efforts

The time discretized control schemes of Figs. 1 and 2 are compared in terms of computational efforts and robustness to parameters variation. Such a comparison is performed by considering a modified structure for the open loop VI estimator, whose integration operation is approximated through low-pass filtering [5], as shown in Fig.3. In fact, the pure integration is affected by drift effects associated to possible offsets into the measured electrical variables. The use of a low-pass filtering algorithm with cut off frequency equal to ω_0 is a required step in practical implementations and allows to obtain a more robust solution. Of course, such a modification will require additional code in the firmware that is conveniently considered in this paper.

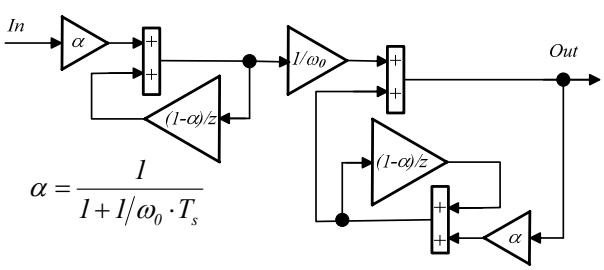

Fig. 3- Modified integration algorithm

The number of operations is a key aspect to consider when the microprocessor resources are limited.

As shown in Table I, the proposed Luenberger observer requires almost double operations to perform the rotor position estimation with respect the standard VI estimator. However, such an advantage of the VI estimator cannot completely exploited in terms of a smaller T_s , as flux calculation is often not included in a subroutine and runs at the same time step of the vector control. Furthermore, the simplicity of the scheme is paid in terms of robustness to parameters variation. Simulations have been carried out in order to evaluate the errors on the rotor position estimated signal, when the two considered schemes are adopted. The data of the PMSM used in the simulations are indicated in Table II.

Table I Computational efforts

	Add/Sub	*Mul/Div*	*Others*	*Total*
VI estimator	4	7	2	13
Luenberger observer	15	10	4	29

Table II -PMSM Data

Number of phases	3
Rated Power	0,44 kW
Rated Voltage	230 V
Max Frequency	330Hz
Max Speed	5000 rpm
Rated Current	3.9 A
Pole Pairs	4
Rotor Inertia	34 μ $k_g m^2$

The results shown in Figs. 4 and 5confirm that the rotor position estimation obtained by the Luenberger observer exhibits a considerably reduced dependence on the stator resistor variation in a wide speed range, while, both structures are quite sensible to synchronous inductance variations.

The rotor position has been obtained respectively from $\hat{\lambda}_{PM\alpha\beta}$ for the VI and from $\hat{e}_{\alpha\beta}$ for the Luenberger scheme, by using an algorithm similar to the resolver-to-

digital conversion scheme, as shown in Fig. 6. A phase shift equal to $\pi/2$ has to be added if EMFs are considered.

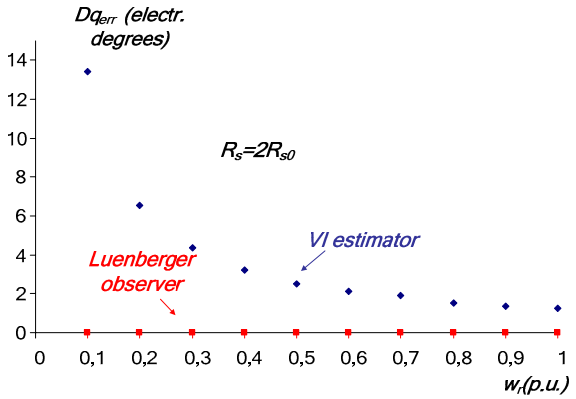

Fig.4- Rotor position error due to stator resistor variation vs speed, 1Nm, for both techniques.

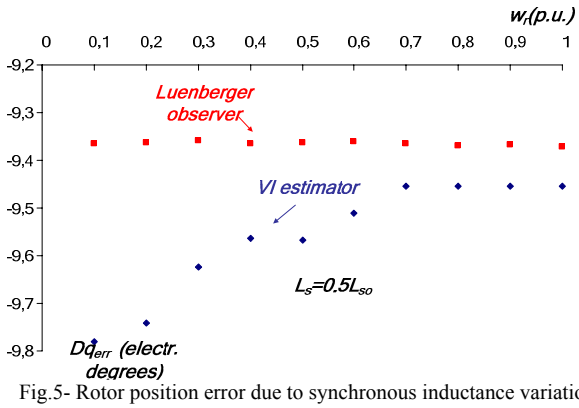

Fig.5- Rotor position error due to synchronous inductance variation vs speed, 1Nm, for both techniques.

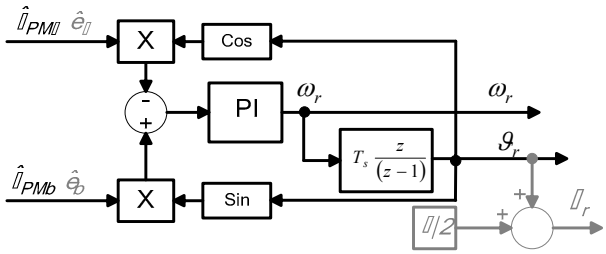

Fig. 6- Rotor position and speed detection scheme.

In Fig. 7 it can be noticed an almost proportional relationship between the synchronous inductance and rotor position errors.

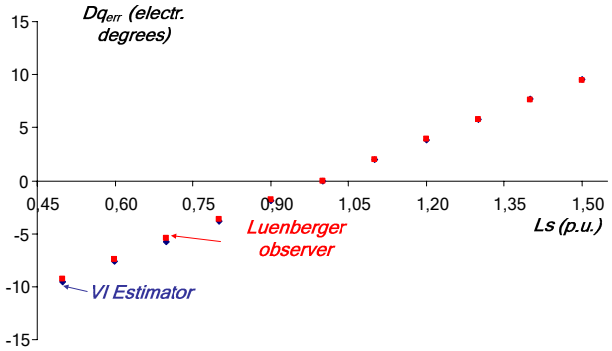

Fig.7- Rotor position error due to synchronous inductance variation, at 2040rpm, 1Nm, for both techniques.

Such results have been obtained either by considering an inductance variation due to saturation either in the case of an incorrect inductance value adopted in the model.

III. Experimental Validation

From the previous section it is clear that the only limitation of the Luenberger observer is represented by the computational resources required to its implementation. The algorithms have been tested on the same PMSM used for simulations. The motor has been connected to a dynamometer and controlled through a ST evaluation control board STM3210B-MCKIT.In Fig. 8 is shown a picture of the experimental setup.

A. Currents and voltages measurement

The three phase currents are measured through three shunt resistors by exploiting properly synchronization of the fast A/D conversions with the generated PWM signals. In fact, only two out of three phase currents have been sampled and the choice was made to satisfy the following rules:

- current sampling is executed only when the corresponding low side switch is on;
- samplings are performed on the two phases that have the longest low side duty cycles thus achieving the longest available sampling times;
- inside the resulting suitable time slots, the very moment to start the ADC conversion must take into account the electrical noises to be avoided (due to commutations of the power stage), the settling time required by the op-amp such as the rise time and, of course, the dead times;
- two currents chosen have been sampled contemporaneously (dual ADC required).

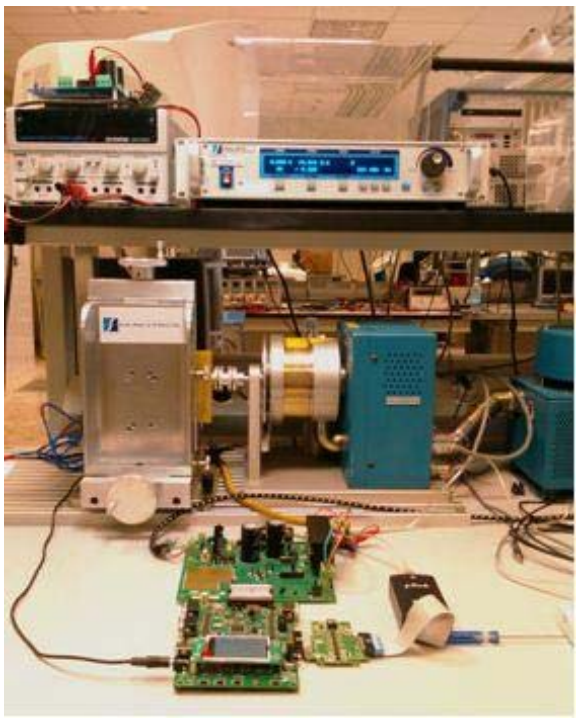

Fig.8 - Experimental setup

Such a strategy is possible only with a dual ADC peripheral which is able to sample the current quickly and deterministically almost everywhere along the PWM period. In Fig. 9 is shown how the sampling synchronization is performed.

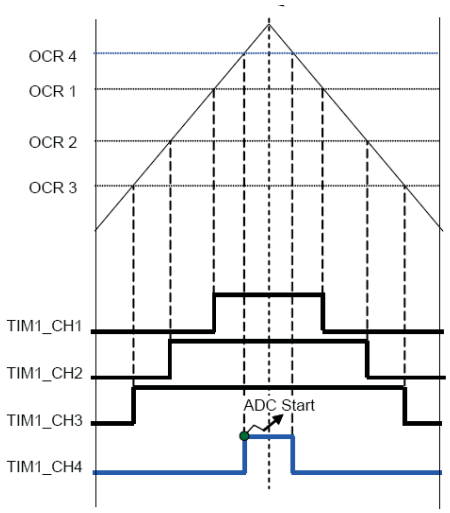

Fig. 9 - PWM and ADC synchronization, OCx- uC Output Compare Registers, TIM1_CHx (x=1,2,3) - low side commands

The phase voltage measurements have been performed suitably combining the DC bus voltage instantaneous value to the voltage references $v_{\alpha\beta s}$. In this way, the DC bus voltage ripple due to the capacitor can be effectively taken into account. The block diagram of the tested sensorless control is shown in Fig. 10.

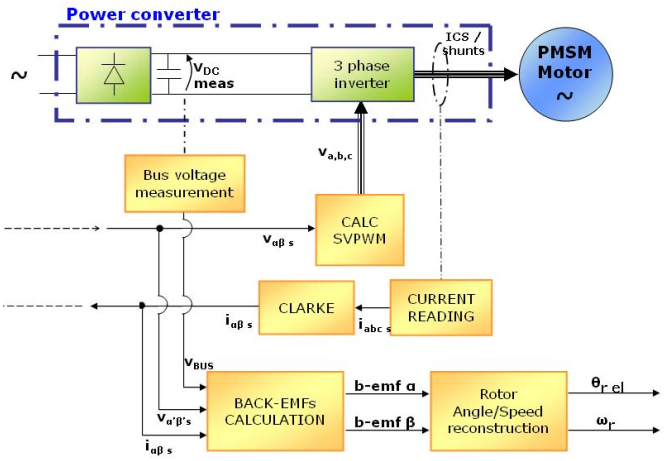

Fig.10 -Sensorless algorithm block diagram

B. *Experimental tests*

Validation of the schemes proposed in Figs 1 and 2 have been performed with the experimental setup of Fig. 8. Both sensorless algorithms have been tested at steady state, in transient and by supposing parameter variations. The results are shown in Figs. 11÷18.In particular, Fig. 11 shows the steady state rotor position, speed and fluxes estimation obtained by means of the VI open loop estimator and Figs. 12, 13 and 14 show the implementation of the Luenberger observer.

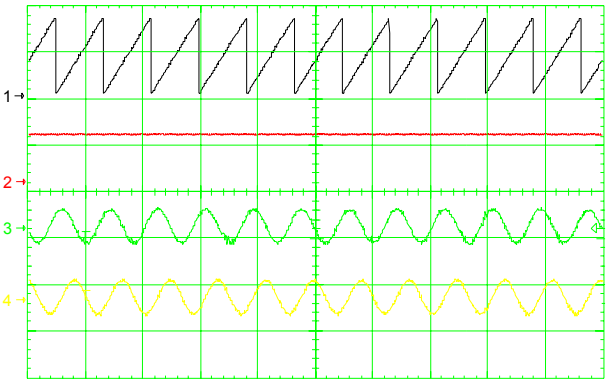

Fig. 11- CH1) Estimated rotor angle [πrad/div], CH2). Estimated rotor speed [80rad/s div], CH3) and CH4) estimated PM fluxes [0,7Wb/div], Time [40 ms/div]

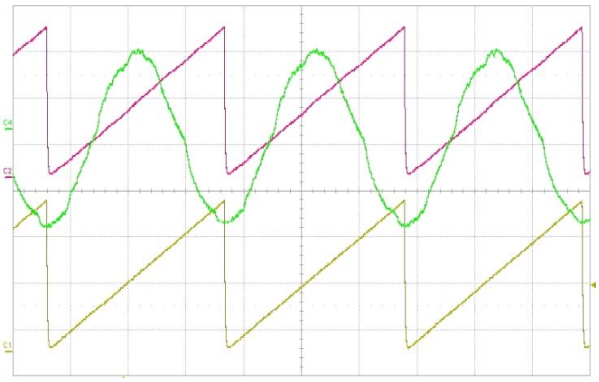

Fig. 12- CH1) Measured rotor angle [2,094rad/div], CH2). Estimated rotor angle [2,094rad/div], CH3) stator phase currents [500mA/div], Time [100 ms/div]

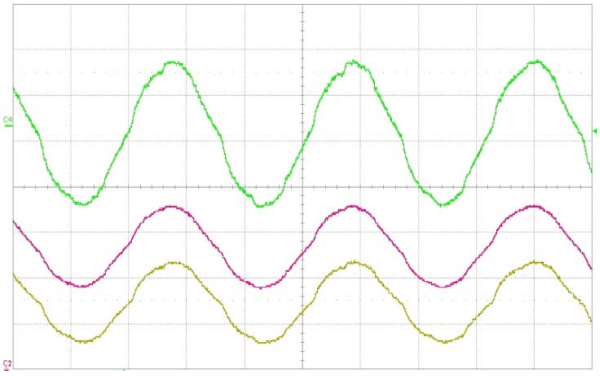

Fig. 13-Current measurements: CH1) Measured phase current (shunt resistor) [500mA/div], CH2). Observed phase current [500mA/div], CH3) Measured phase current [500mA/div], Time [10 ms/div]

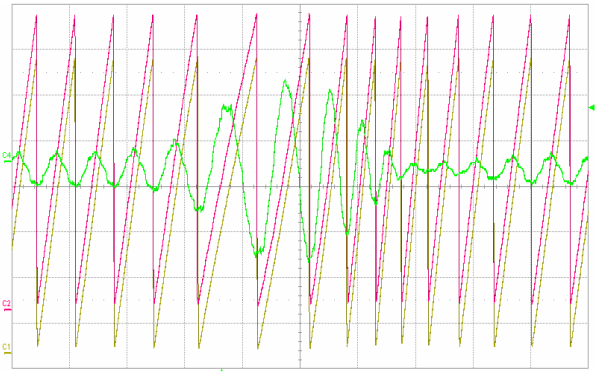

Fig. 14-Transient Analysis: CH1) Measured rotor angle [1,047rad/div], CH2). Estimated rotor angle [1,047rad/div], CH3) stator phase currents [500mA/div], Time [500 ms/div]

Fig.12 deals with the steady state estimated flux angle, Fig. 13 the measurements performed by the shunt resistor and Fig. 14 a transient analysis when a torque disturbance equal to the rated value has been applied.

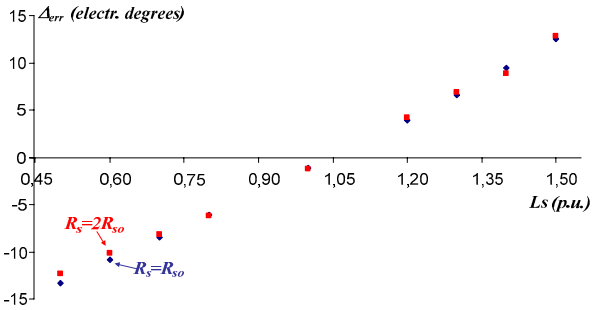

Fig.15- Rotor position error due to parameters variation, at 2040rpm, 1Nm load torque

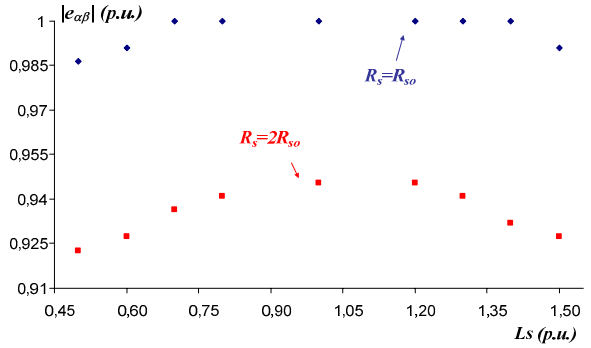

Fig.16- Amplitude variation of back emf due to parameters variation, at 2040rpm, 1Nm load torque

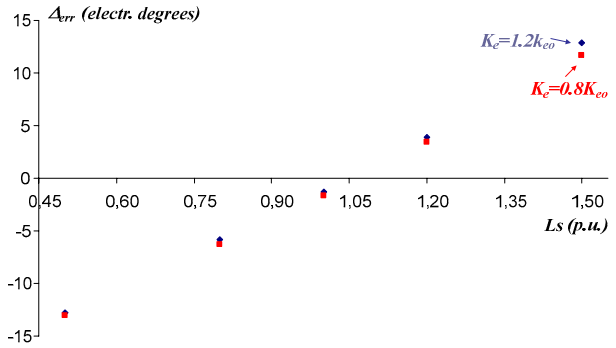

Fig.17- Rotor position error due to back emf constant variation, at 2040rpm, 1Nm load torque

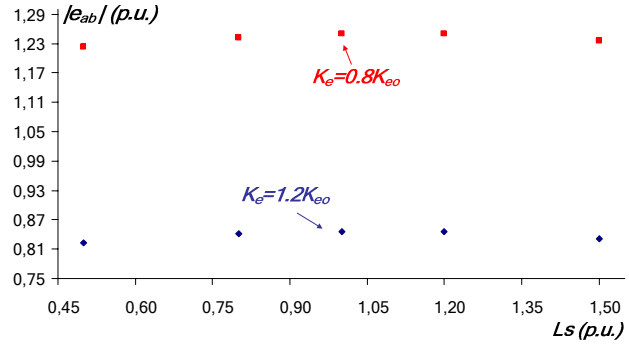

Fig.18- Amplitude variation of back emf due to back emf constant variation, at 2040rpm, 1Nm load torque.

Figs. 15÷18 deals with parameter variations. Fig. 15 confirms the parameters sensitivity of the Luenberger observer as obtained by simulations. As previously stated, a wrong evaluation of the stator resistor value or a temperature variation not effects the estimation of the back EMFs. On the contrary, such a estimation is influenced by synchronous inductance variations, as shown in Fig. 16. In this case, the estimation error is considerable, especially when the machine operates at high saturation level or, with opposite sign, in case of a incorrect evaluation of the synchronous inductance.

Observed back EMF amplitudes depend on parameters value as well; the results of the experimental tests shown in Figs. 17 and 18, allow stating that such an influence can be considered negligible, since no substantial changes occur in the maximum value of the sinusoidal waveforms $e_{\alpha\beta}$. Since both algorithms are tested on a 32 bit fixed point microprocessor, a suitable normalizing procedure has been adopted to exploit the maximum resolution. According to such a procedure, the rated values of $e_{\alpha\beta}$ are indicated in Figs. 17 and 18 as K_e. The tests show a possible mistake during this normalizing procedure and that the variation of the parameter K_e does not affects the phase and amplitude of $e_{\alpha\beta}$.

IV. Conclusions

The paper describes a comparison between some different high-performance low-cost-implementation techniques for the estimation of the rotor flux in medium-high speed permanent magnet motor drives. Some implementation differences between a classical open loop rotor flux estimator based on the voltage model, and a more complex Luenberger rotor flux observer are pointed out. The two algorithms have been compared either in simulation and experimentally, by means of a STM32microcontroller. Although the VI estimator can potentially run faster than the Luenberger observer, the tests reported in the paper show that the more complex scheme assures better robustness on parameter variation.

REFERENCES

[1] B. Bose, “power Electronics and Variable Frequency Drives”, IEEE Press Piscataway, NJ USA, 1997.

[2] M. Tursini, R. Petrella, F. Parasiliti, “Adaptive sliding-mode observer for speed-sensorless control of induction motors”, IEEE Transactions on Industry Applications, vol. 36, n. 5, Sept.-Oct. 2000,pp.1380-1387.

[3] P.L. Jansen, R.D. Lorenz, “A physically insightful approach to the design and accuracy assessment of flux observers for field oriented induction machine drives”, IEEE Transactions on Industry Applications, vol. 30, n. 1, Jan.-Feb. 1994 pp. 101-110.

[4] S.A. Luiz, S. R Silva, B.R. Menezes, “Assessment of flux observer performance for induction motor drive”, Proc. of IECON 97, volume 2, 9-14 Nov. 1997, pp. 494-499

[5] K. D. Hurst, T. G. Habetler, G. Griva, F. Profumo, ”Zero-Speed Thacoless IM Torque Control: Simply a Matter of Stator Voltage Integration”, IEEE Transaction on Industry Applications, 1998, July/August, vol. 34, n. 4, pp.:790-795.